UR 2000-1

I-28266

PPPL-2380

UC20-F

156
10-16-86 JS (2)

(35)

PPPL-2380

PPPL--2380

DE87 000678

DISRUPTION CHARACTERISTICS IN PDX WITH LIMITER AND DIVERTOR DISCHARGES

By

P. Couture and K. McGuire

SEPTEMBER 1986

PLASMA PHYSICS LABORATORY

PRINCETON UNIVERSITY

PRINCETON, NEW JERSEY

PREPARED FOR THE U.S. DEPARTMENT OF ENERGY, UNDER CONTRACT DE-AC02-76-CHO-3073.

DISRUPTION CHARACTERISTICS IN PDX WITH LIMITER AND DIVERTOR DISCHARGES

P. Couture* and K. McGuire

Plasma Physics Laboratory, Princeton University

Princeton, New Jersey 08544

ABSTRACT

A comparison has been made between the characteristics of disruptions with limiter and divertor configurations in PDX. A large data base on disruptions has been collected over four years of machine operation, and a total of 15,000 discharges are contained in the data file. It was found that divertor discharges have less disruptions during ramp up and flattop of the plasma current. However, for divertor discharges a large number of fast, low current disruptions take place during the current ramp down. These disruptions are probably caused by the deformation of the plasma shape.

DISCLAIMER

This report was prepared as an account of work sponsored by an agency of the United States Government. Neither the United States Government nor any agency thereof, nor any of their employees, makes any warranty, express or implied, or assumes any legal liability or responsibility for the accuracy, completeness, or usefulness of any information, apparatus, product, or process disclosed, or represents that its use would not infringe privately owned rights. Reference herein to any specific commercial product, process, or service by trade name, trademark, manufacturer, or otherwise does not necessarily constitute or imply its endorsement, recommendation, or favoring by the United States Government or any agency thereof. The views and opinions of authors expressed herein do not necessarily state or reflect those of the United States Government or any agency thereof.

Permanent Address: *IREQ Institut de recherche d'Hydro-Quebec, Canada.

MASTER

DISTRIBUTION OF THIS DOCUMENT IS UNLIMITED

I. INTRODUCTION

The objective of this report is to study the characteristics of disruptions with limiter and divertor configurations in PDX. Disruption characteristics are of interest because of the large forces produced by the disruption. This information is critical to the design of vacuum vessels and poloidal field systems for future machines. Some of the problems caused by the plasma current decay could be (a) tilting forces on the toroidal field coils, (b) over-voltage in the poloidal coils, (c) torques on structures inside the vacuum vessel, and (d) arcing problems due to the large voltages induced by the current jump at a disruption.

In this report we will not make a distinction between neutral-beam-heated and ohmic-heated disruptions. The shape of diverted discharges is similar to circular discharges. On PDX, a large data base on disruption characteristics has been collected over 4 years of machine operation. A total of 15,000 discharges are contained in the data file.

For this study, we will consider discharges from the years 1982 to 1983, (#46291 to #63395). This range of shot numbers corresponds to 3542 limiter discharges and 3451 diverted discharges. The year 1982 corresponds mainly to the beta push in the limiter and divertor discharges, and in 1983 to the H-mode study in the diverted discharges. The limiter discharges included the inner armor limiter, rail limiter, and scoop limiter.

II. EXPERIMENTAL PROCEDURE

For each discharge, 23 parameters are recorded. For example, R, A, B_ϕ, gas species, configuration (limiter, divertor), $\beta_\theta + \ell_i/2$, loop voltage, $\bar{n}_e$, I_p before, during, and after disruption, and the current decay rate $\Delta I/\Delta T$, etc. This data can then be displayed in different forms, i.e., histograms or

2D and 3D plots [1,2]. For the purpose of the data base, a disruption is defined as a sharp rise in the plasma current, followed by a decrease in current. This means that both major and minor disruptions are detected. Disruptions are detected during a discharge by using the plasma current, I_p, as a monitor. The I_p current is measured with a Rogowski coil. The signal is corrected for coil can eddy current. The time constant of the coil can is L/R = 1.5 ms. The discharge is divided into 100 ms portions, and an increase of I_p followed by a decrease in I_p is searched for in that segment. When a disruption is detected, the time in milliseconds and the current in kiloamps before, during, and after the event are stored in the data file. The following gives a brief outline of the procedure.

Three times and three currents are recorded for each disruption (see Fig. 1). The first (I_{p1}, T_1) is at the start of the disruption, just before the plasma current jump. The second time (I_{p2}, T_2) is at the peak of the plasma current jump. The final time recorded is at the end of the current decrease (I_{p3},T_3). Each discharge may have many disruptions.

A simple Fortran routine is used to evaluate $\Delta I/\Delta T$, which is defined as $-(I_{p3} - I_{p2})/(T_3 - T_2)$. The data acquisition system samples at 10 kHz. Other quantities recorded are:

Rise time = T_2-T_1

Fall time = $T_3- T_2$

Percentage current jump = $100 \times (I_{p2} - I_{p1})/I_{p1}$

Delta I_p = $I_{p1}-I_{p3}$

Lowest current = I_{p3}

Then, the maximum derivative between T_1 and T_2 as well as a similar minimum derivative are calculated by a scientific software package (IMSL routine).

With the analysis program, four different decay rates after the disruption can be studied: the current decay after the first disruption, the average $\Delta I/\Delta T$ for a series of disruptions, the highest $\Delta I/\Delta T$ during a series of disruptions, or all of the decay rates after the disruptions during a discharge [2].

III. GENERAL CHARACTERISTICS

Figures 2(a) and 2(b) show the plasma current as a function of the time in the discharge at which the disruption occurred: (a) is for limiter discharges and (b) is for the divertor discharges. The data shown in Fig. 2 are for the highest $\Delta I/\Delta T$ (kA/ms) during a discharge. The outstanding difference between the figures is the large number of disruptions which occur after 800 ms, with low plasma current in the divertor discharges. From Figs. 2(c) and 2(d), it is observed that some of the late disruptions in the divertor configuration can have fast decay rates, i.e., high $\Delta I/\Delta T$ (kA/ms).

Plots of $\Delta I/\Delta T$ (kA/ms) versus plasma current are shown in Figs. 2(e) and 2(f) for circular and divertor plasmas, respectively. It is found that a linear type dependence of $\Delta I/\Delta T$ versus I_p could describe a large percentage of the data. The relationship for circular discharges is $\Delta I/\Delta T$ (kA/ms) = I_p(kA)/20; however, some disruptions have $\Delta I/\Delta T$ (kA/ms) = I_p (kA)/7.5, especially at a higher current. They correspond to inner wall limiter discharges [1]. For divertor discharges, the situation is somewhat different. The linear dependence still exists, but there is a large scatter of data. However, two classes of disruptions can be identified. For high currents, a scaling like $\Delta I/\Delta T$ (kA/ms) = I_p (kA)/40 fits well and at low currents, a scaling of $\Delta I/\Delta T$ (kA/ms) = I_p (kA)/2.5 is more appropriate. There is, however, a large scatter of data between these two limits. Nevertheless,

divertor discharges at low current can disrupt fast, i.e., $\Delta I/\Delta T$ (kA/ms) = I_p (kA)/2.5. This class of disruption is missing in the limiter discharges.

The $\beta_\theta + \ell_i/2$ signal versus "time of disruption" is shown in Figs. 3(a) and 3(b). The low current divertor disruptions that occur late in the discharge (i.e., after 800 ms) are characterized by high $\beta_\theta + \ell_i/2$, with values up to 5 in some cases because a is kept fixed. However, there is an uncertainty in this value of $\beta_\theta + \ell_i/2$ due to eddy currents.

Histograms of the loop voltage before the first disruption of each shot are shown for divertor and limiter configurations in Figs. 3(c) and 3(d). The loop voltage is on the average lower for the divertor configuration. A more striking difference between the two figures is the large number of disruptions with negative loop voltage at the time of the disruption for the divertor configuration. These disruptions with negative loop voltage, occur toward the end of the discharge when the plasma current is being ramped down by imposing a negative voltage on the plasma. These negative loop voltage disruptions occur when the plasma current is low as shown in Figs. 3(e) and (f) where the circular and divertor disruptions are compared.

If a plot is made of $\Delta I/\Delta T$ versus current for divertor disruptions with negative loop voltage (Fig. 4a), there appear to be two different decay times, one with $I_p/40$ kA/ms and the other with $I_p/2.5$ kA/ms. A detailed study of these two groups of late disruptions in divertor discharges will be discussed later.

During the transport phase of a major disruption (see Fig. 4b for disruption phases), the plasma current increases rapidly. This increase in current is measured as a percentage of the total current, and the results are shown in Figs. 5(a) and 5(b) for circular and divertor discharges, respectively. From the histograms it is observed that the mean percentage

current jump is 12% for the circular configuration and only 8% for the divertor discharges. However, with the divertor configuration, there are quite a lot of disruptions with current jumps above 20%. These high percentage current jump discharges happen mainly at disruptions with $\Delta I/\Delta T = I_p/2.5$ kA/ms, which occur toward the end of the discharge.

Histograms of negative voltage spikes at the disruption are shown in Figs. 5(c) and 5(d) for circular and divertor discharges, respectively. The peak of the distribution is centered at -40 volts and the distribution has a long tail for the divertor configuration. The circular plasmas have a peak in the distribution at about -15 volts. In the case of divertor discharges, there are some disruptions with negative voltage spikes as high as 1 keV.

When a plot of the negative voltage spike versus current for circular plasmas is made, it is clear that there may be some correlation between amplitude of negative voltage spike and I_p, i.e., $V_{spike} < 0.75\ I_p$ [see Fig. 5(e)]. For divertor plasmas, the situation is somewhat different, especially since large negative voltage spikes are observed at low plasma current [see Figure 5(f)]. These low current disruptions are the special case of disruptions which occur late in the discharge.

For limiter discharges the negative voltage spikes lie between 0 to -150 V for a percentage current jump between 5 to 18%. For the diverted discharges the spread of values is larger with negative voltage spikes up to -400 V and percentage current jumps up to 40%. We have seen in Fig. 3(d) that diverted discharges have more disruptions with negative loop voltage than limiter discharges and that these disruptions can be divided mainly into two categories. The first one is with low current I_p <110 kA and $\Delta I/\Delta T = I_p/2.5$ and the second one with $\Delta I/\Delta T = I_p/40$ kA/ms. In the next section we will look more closely at the characteristics of these disruptions.

IV. COMPARISON OF TWO CLASSES OF DISRUPTIONS FOR DIVERTED DISCHARGES WITH NEGATIVE LOOP VOLTAGE

These disruptions happen at the end of the diverted discharge when the current is ramped down and the loop voltage is driven negative [see Figs. 6(a), (b)]. The first disruption in a discharge with high $\Delta I/\Delta T = I_p/2.5$ kA/ms happens later in time, Fig.6(a), than the first disruption in a discharge with low $\Delta I/\Delta T = I_p/40$ kA/ms [see Fig. 6(b)]. The current for disruptions with $\Delta I/\Delta T = I_p/2.5$ kA/ms, ranges between 0 and 110 kA [see Fig. 6(c)] and for $\Delta I/\Delta T = I_p/40$ kA/ms between 60 and 400 kA [see Fig. 6(d)]. However, the low current disruptions have a high $\Delta I/\Delta T = I_p/2.5$ kA/ms and the high current disruptions have a low $\Delta I/\Delta T = I_p/40$ kA/ms [see Figs. 6(e),(f)]. The low current disruptions have a higher q_a than the high current disruptions. The $\beta_\theta + \ell_i/2$ is also much higher for the low current disruptions than for those with high current. The histograms of percent current jump do not show a peak for disruptions with low current but show a wider spread compared to disruptions with higher current which have a peak around 8% [see Figs. 7(a),(b)]. Finally, one of the most obvious differences between these two kinds of disruptions is the decay time. The low current disruptions decay in a few msecs compared to a much longer time for the high current discharges [see Figs. 7(c),(d)].

V. DIVERTOR DISRUPTIONS WITH POSITIVE LOOP VOLTAGE

Divertor disruptions with positive loop voltage show no clear dependence of $\Delta I/\Delta T$ with plasma current [Fig. 8(a)]. However, it appears that the low $\Delta I/\Delta T$ kA/ms disruptions have a small current decay, i.e., $\Delta I_p < 140$ kA, which suggests that these discharges did not have a major disruption. Nevertheless,

the disruptions with $\Delta I/\Delta T$ > 18 kA/ms appear to be disruptions which had a high current decay ΔI_p > 200 kA and thus were fast major disruptions [Fig. 8(b)].

VI. DISCUSSION

Disruptions were studied in both limiter and divertor discharges. The limiter discharges included inner wall, rail, and scoop limiters. Comparison between limiter and divertor discharges has shown that divertor discharges have more disruptions with high $\Delta I/\Delta T$ and large negative voltage spikes, and have lower loop voltages than limiter disruptions. The main difference between divertor and limiter operation is the higher number of disruptions for divertor discharges during the ramp down of the plasma current [3]. If we neglect the disruptions during ramp down, we can say that divertor operation looks similar to limiter discharges except that the number of disruptions is much lower with divertor operation [see Figs. 3(c),(d)]. Two classes of disruptions have been observed for divertor discharges during current ramp down. The first type includes a wide range of plasma currents and is characterized by a small $\Delta I/\Delta T = I_p/40$ kA/ms. This class of slow disruption does not present any risk for the life of a tokamak. The second class of disruption which happens at the end of a discharge when the current is less than 110 kA and which is characterized by $\Delta I/\Delta T = I_p/2.5$ kA/ms could cause problems for the tokamak because $\Delta I/\Delta T$ is relatively high. These high q discharges have also high $\beta_\theta + \ell i/2$, and are directly caused by the divertor operation. Equilibria calculations were run for one of those high $\Delta I/\Delta T$ disruptions at three different times (see Fig. 9). The first one was run at peak current 600 ms, the second one was run at 900 ms, and the last one at 930 ms or 1 ms before disruption. We see clearly that the discharge shrinks with

time. This could be the cause of the disruption, but we cannot exclude the interaction of the separatrix with the armor plate or a combination of both phenomena to produce the fast disruption. The lack of information at the end of the discharge makes further study difficult. Note the strong divertor field toward the end of the discharge.

VII. CONCLUSION

From the analysis of disruptions in PDX it is found that it is easier to avoid disruptions during ramp up and flattop of the plasma current in divertor configurations. However, disruptions during the current ramp down may present a problem for a bigger machine. These disruptions are probably caused by the deformation of plasma shape. However, the interaction of the separatrix with the inner wall or the armor plate on the inner wall during current ramp down or a combination of both phenomena may also be causing the disruptions. A possible solution to avoid those disruptions with $\Delta I/\Delta T = I_p/2.5$ kA/ms is to ramp down the divertor's coil current at the same speed as the plasma current.

ACKNOWLEDGMENTS

The authors would like to thank Kees Bol for fruitful discussions, Gary Hay for setting up the disruption data base, and H. Fishman for running the equilibrium field code. We also want to thank the PDX group, and the PDX technical crew for assistance and support in these experiments.

This work supported by U.S. Department of Energy Contract No. DE-AC02-76-CHO-3073.

REFERENCES

[1] K. McGuire, D. Buchenauer, P. Couture, R. Izzo, K. Kawahata, D. Monticello, K. Okano, and N. Sauthoff, "Major Disruption Characteristics with a Toroidal Limiter in PDX," in Symposium on Energy Removal and Particle Control in Toroidal Fusion Devices (July 1983). J. Nuc. Mater. 121 (1984) 329.

[2] G. Hay et al., Bull. Am. Phys. Soc. 26 (1981) 865.

[3] P. Couture et al., Bull. Am. Phys. Soc. 28 (1983) 1174.

FIGURE CAPTIONS

Fig. 1 Schematic of time evolution of plasma current during a disruption.

Fig. 2a Plot of plasma current versus the time of disruption for the highest $\Delta I/\Delta T$ in a discharge for limiter discharges.

Fig. 2b Plot of plasma current versus the time of disruption for the highest $\Delta I/\Delta T$ in a discharge for divertor discharges.

Fig. 2c Plot of $\Delta I/\Delta T$ versus the time of disruption for the highest $\Delta I/\Delta T$ in a discharge for limiter discharges.

Fig. 2d Plot of $\Delta I/\Delta T$ versus the time of disruption for the highest $\Delta I/\Delta T$ in a discharge for divertor discharges.

Fig. 2e Plot of $\Delta I/\Delta T$ versus plasma current for the highest $\Delta I/\Delta T$ in a discharge for limiter discharges.

Fig. 2f Plot of $\Delta I/\Delta T$ versus plasma current for the highest $\Delta I/\Delta T$ in a discharge for divertor discharges.

Fig. 3a Plot of $\beta_\theta + \ell i/2$ versus time of disruption for the highest $\Delta I/\Delta T$ in a discharge for limiter discharges.

Fig. 3b Plot of $\beta_\theta + \ell i/2$ versus time of disruption for the highest $\Delta I/\Delta T$ in a discharge for divertor discharges.

Fig. 3c Histogram of loop voltage for the first disruption in a discharge for limiter discharges.

Fig. 3d Histogram of loop voltage for the first disruption in a discharge for divertor discharges.

Fig. 3e Plot of loop voltage versus plasma current for the first disruption in a discharge for limiter discharges.

Fig. 3f Plot of loop voltage versus plasma current for the first disruption in a discharge for divertor discharges.

Fig. 4a Plot of $\Delta I/\Delta T$ versus plasma current for the first disruption in a discharge with negative loop voltage for divertor discharges.

Fig. 4b Disruption phases during a typical major disruption.

Fig. 5a Histogram of percentage of current jumps for all disruptions in a discharge for limiter discharges.

Fig. 5b Histogram of percentage of current jumps for all disruptions in a discharge for divertor discharges.

Fig. 5c Histogram of negative voltage spikes for all disruptions in a discharge for limiter discharges.

Fig. 5d Histogram of negative voltage spikes for all disruptions in a discharge for divertor discharges.

Fig. 5e Plot of negative voltage spike versus plasma current for all disruptions in a discharge for limiter discharges.

Fig. 5f Plot of negative voltage spike versus plasma current for all disruptions in a discharge for divertor discharges.

Fig. 6a Histogram of the time of disruption for the first disruption in a discharge for divertor discharges, with negative loop voltage, the plasma current < 110 kA and $\Delta I/\Delta T$ > 5 kA/ms.

Fig. 6b Histogram of the time of disruption for the first disruption in a discharge for divertor discharges, with negative loop voltage, I_p > 60 kA and $\Delta I/\Delta T$ < 15 kA/ms.

Fig. 6c Histogram of plasma current for the first disruption in a discharge for divertor discharges with negative loop voltage I_p < 110 kA and $\Delta I/\Delta T$ > 5 kA/ms.

Fig. 6d Histogram of plasma current for the first disruption in a discharge for divertor discharges with negative loop voltage, I_p > 60 kA and $\Delta I/\Delta T$ < 15 kA/ms.

Fig. 6e Histogram of $\Delta I/\Delta T$ for the first disruption in a discharge for divertor discharges with negative loop voltage I_p <110 kA and $\Delta I/\Delta T$ > 5 kA/ms.

Fig. 6f Histogram of $\Delta I/\Delta T$ for the first disruption in a discharge for divertor discharges with negative loop voltage I_p > 60 kA and $\Delta I/\Delta T$ < 15 kA/ms.

Fig. 7a Histogram of percentage of current jump for the first disruption in a discharge for divertor discharges, with negative loop voltage, I_p < 110 kA and $\Delta I/\Delta T$ > 5 kA/ms.

Fig. 7b Histogram of percentage of current jump for the first disruption in a discharge for divertor discharges with negative loop voltage, I_p >60 kA/ms and $\Delta I/\Delta T$ < 15 kA/ms.

Fig. 7c Histogram of plasma current decay time for the first disruption in a discharge for divertor discharges with negative loop voltage I_p < 110 kA and $\Delta I/\Delta T$ > 5 kA/ms.

Fig. 7d Histogram of plasma current decay time for the first disruption in a discharge for divertor discharges with negative loop voltages, I_p >60 kA/ms and $\Delta I/\Delta T$ < 15 kA/ms.

Fig. 8a Plot of $\Delta I/\Delta T$ versus plasma current for the first disruption in a discharge for divertor discharges with positive loop voltage.

Fig. 8b Histogram of plasma current decay for the first disruption in a discharge for divertor discharges with positive loop voltage.

Fig. 9 Flux plot contours during ramp down of plasma current. Disruption occurred at 931 ms with a plasma current of 65 kA. We see the X point of the separatrix moving down and up, respectively. (A) T = 600 ms, (B) T = 900 ms, and (C) T = 930 ms.

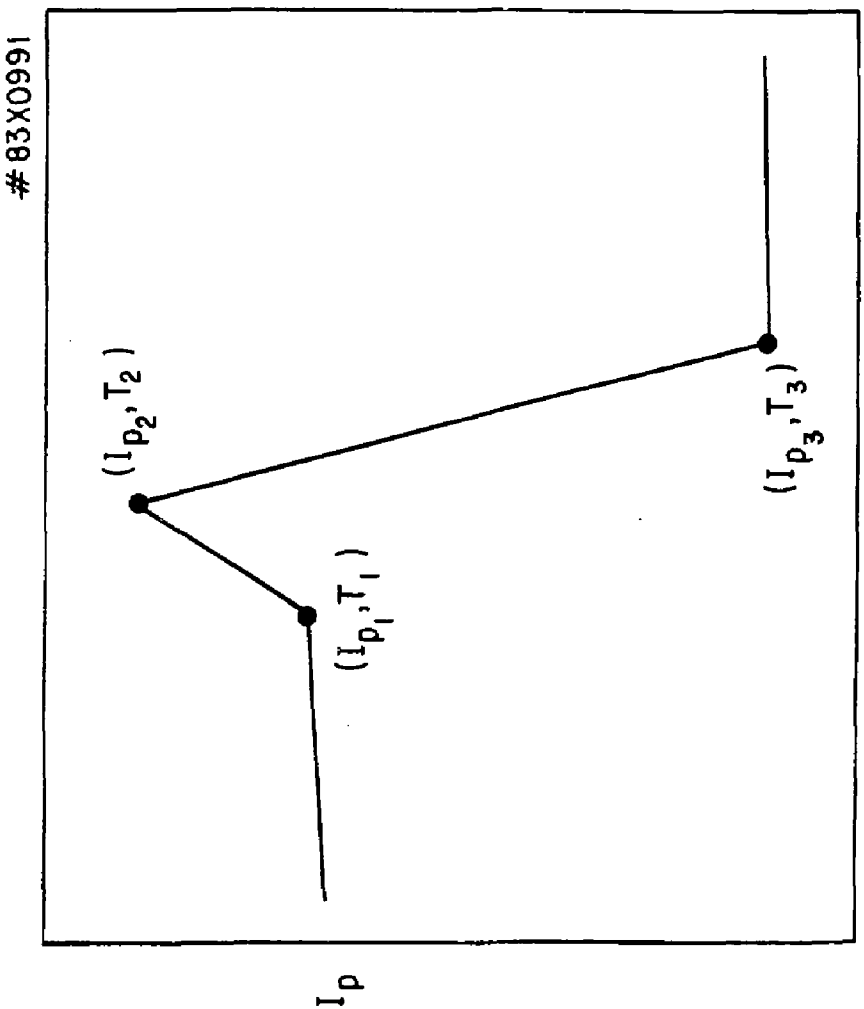

Fig. 1

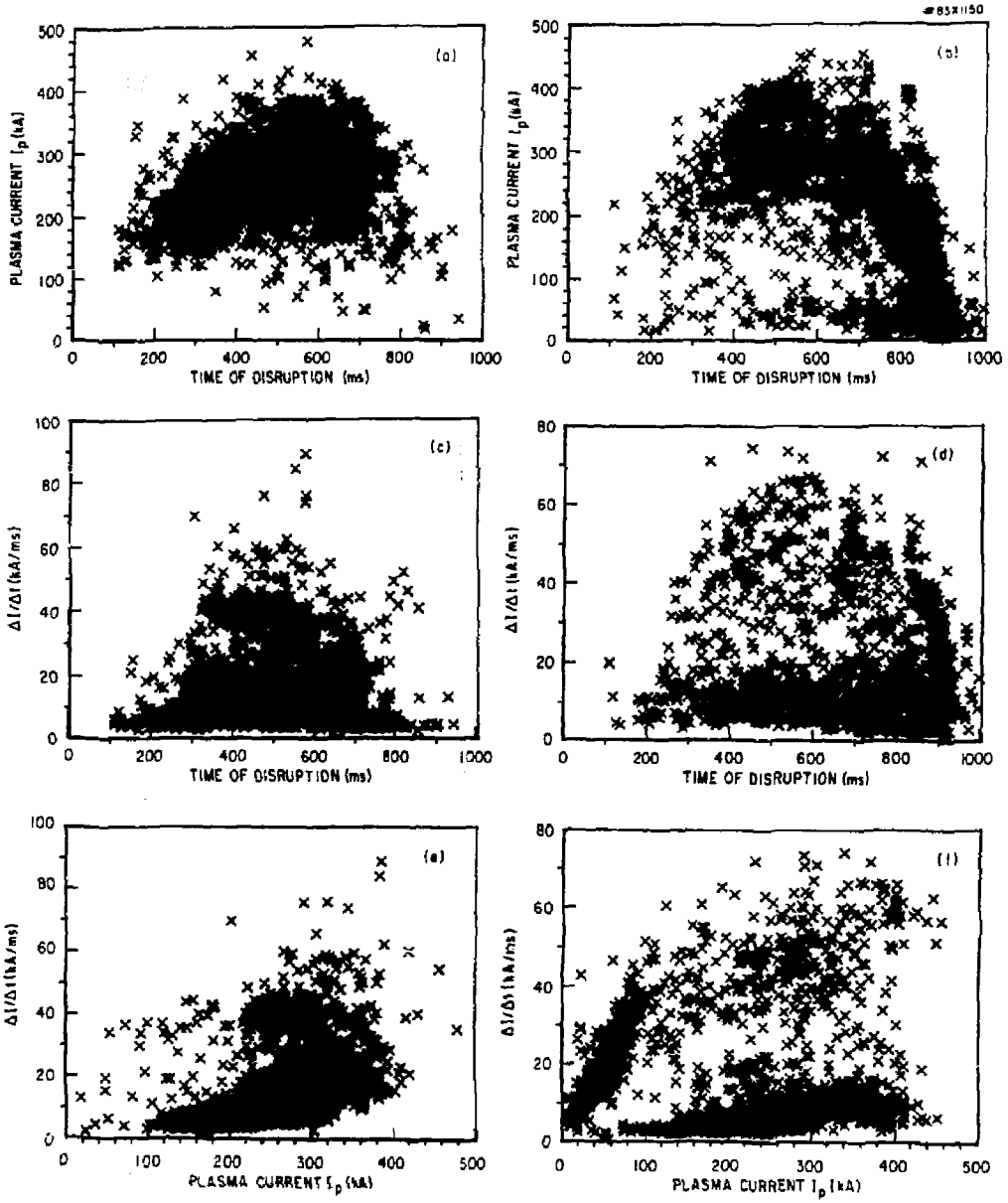
(a)
PLASMA CURRENT I_p (kA)
TIME OF DISRUPTION (ms)
(b)
PLASMA CURRENT I_p (kA)
TIME OF DISRUPTION (ms)
(c)
$\Delta I/\Delta t$ (kA/ms)
TIME OF DISRUPTION (ms)
(d)
$\Delta I/\Delta t$ (kA/ms)
TIME OF DISRUPTION (ms)
(e)
$\Delta I/\Delta t$ (kA/ms)
PLASMA CURRENT I_p (kA)
(f)
$\Delta I/\Delta t$ (kA/ms)
PLASMA CURRENT I_p (kA)

Fig. 2

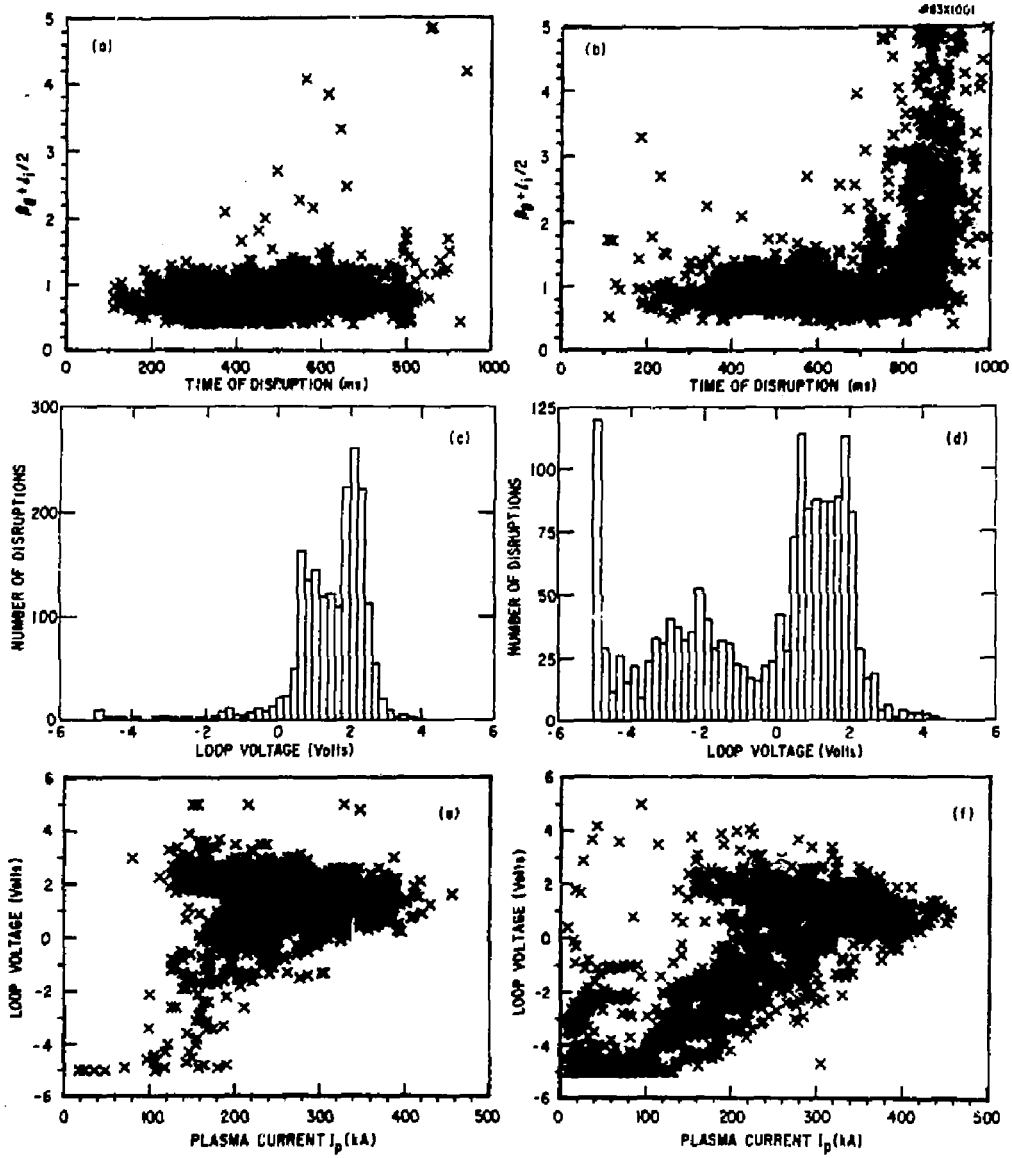
(a)
(b)
(c)
(d)
(e)
(f)
TIME OF DISRUPTION (ms)
NUMBER OF DISRUPTIONS
LOOP VOLTAGE (Volts)
PLASMA CURRENT I_p (kA)

Fig. 3

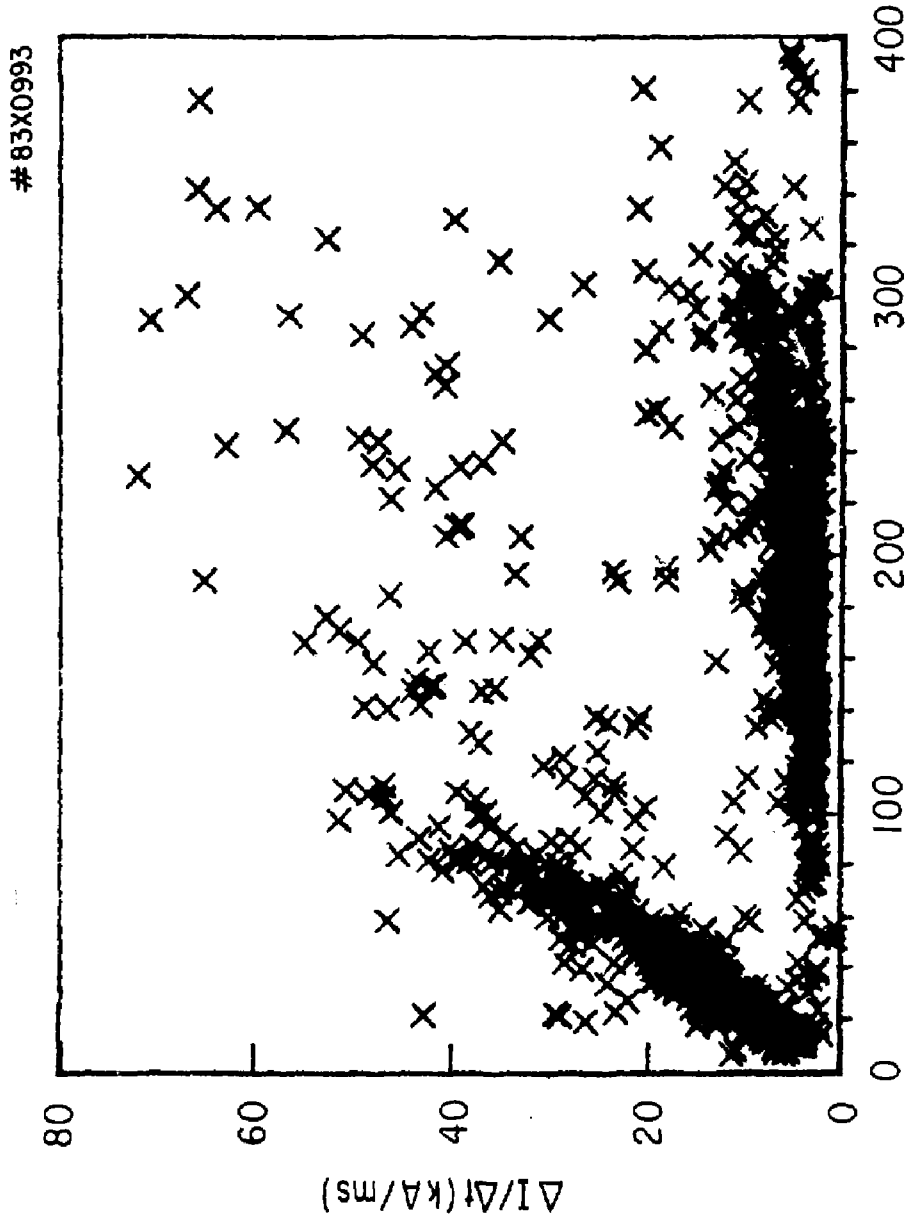
#83X0993
ΔI/Δt (kA/ms)
80
60
40
20
0
0
100
200
300
400
PLASMA CURRENT I_p (kA)

Fig. 4(a)

#83X1037

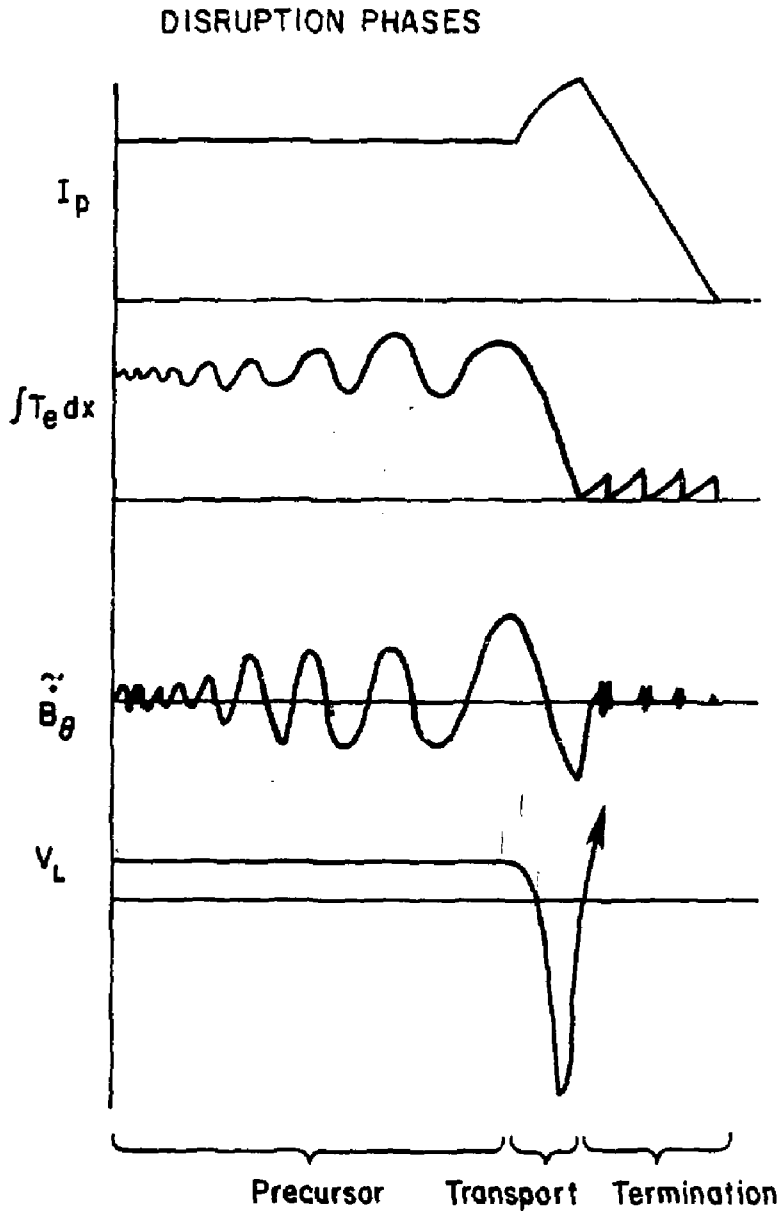

Fig. 4(b)

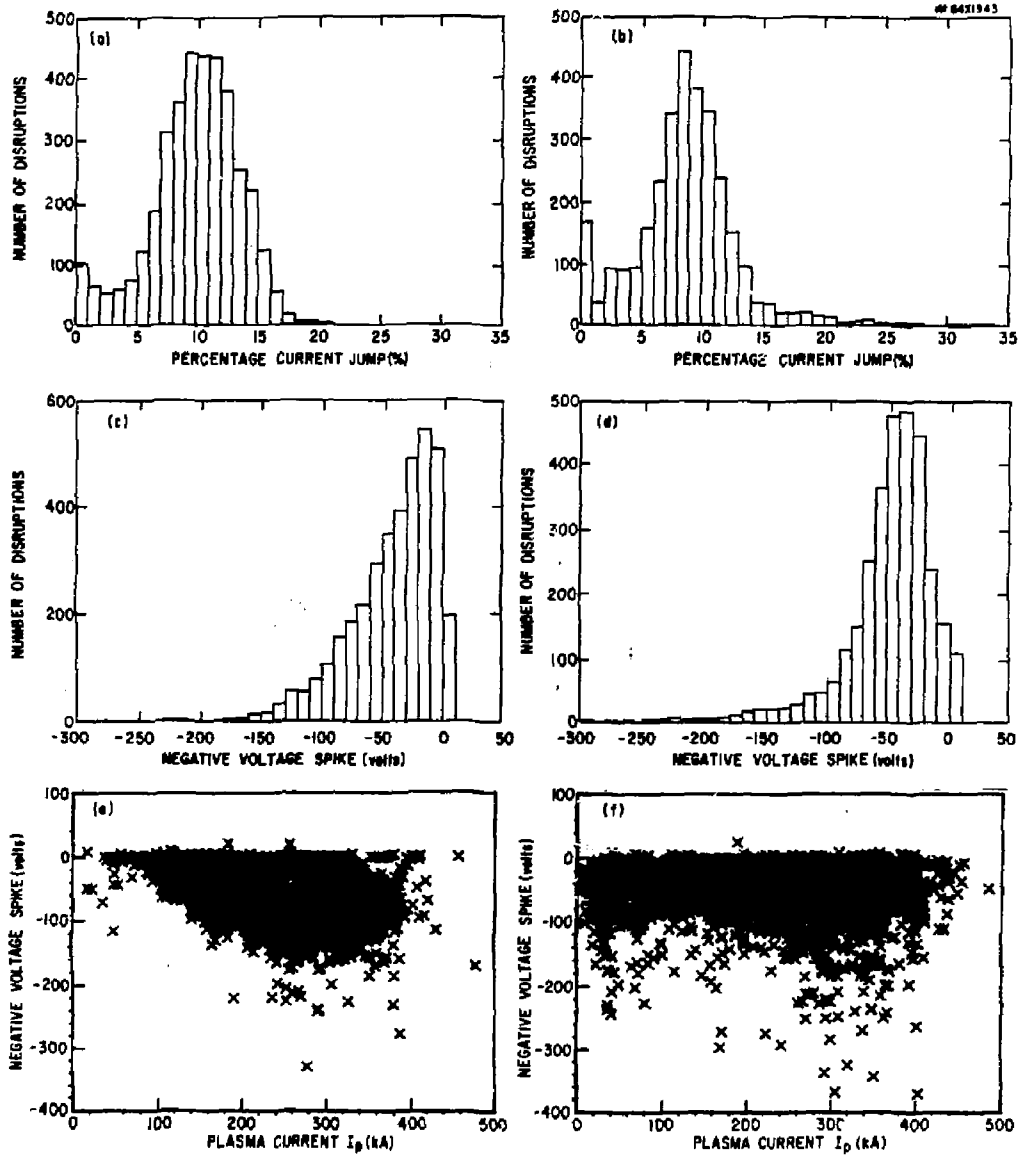
(a)
(b)
(c)
(d)
(e)
(f)
NUMBER OF DISRUPTIONS
PERCENTAGE CURRENT JUMP(%)
NEGATIVE VOLTAGE SPIKE (volts)
PLASMA CURRENT I_p (kA)

Fig. 5

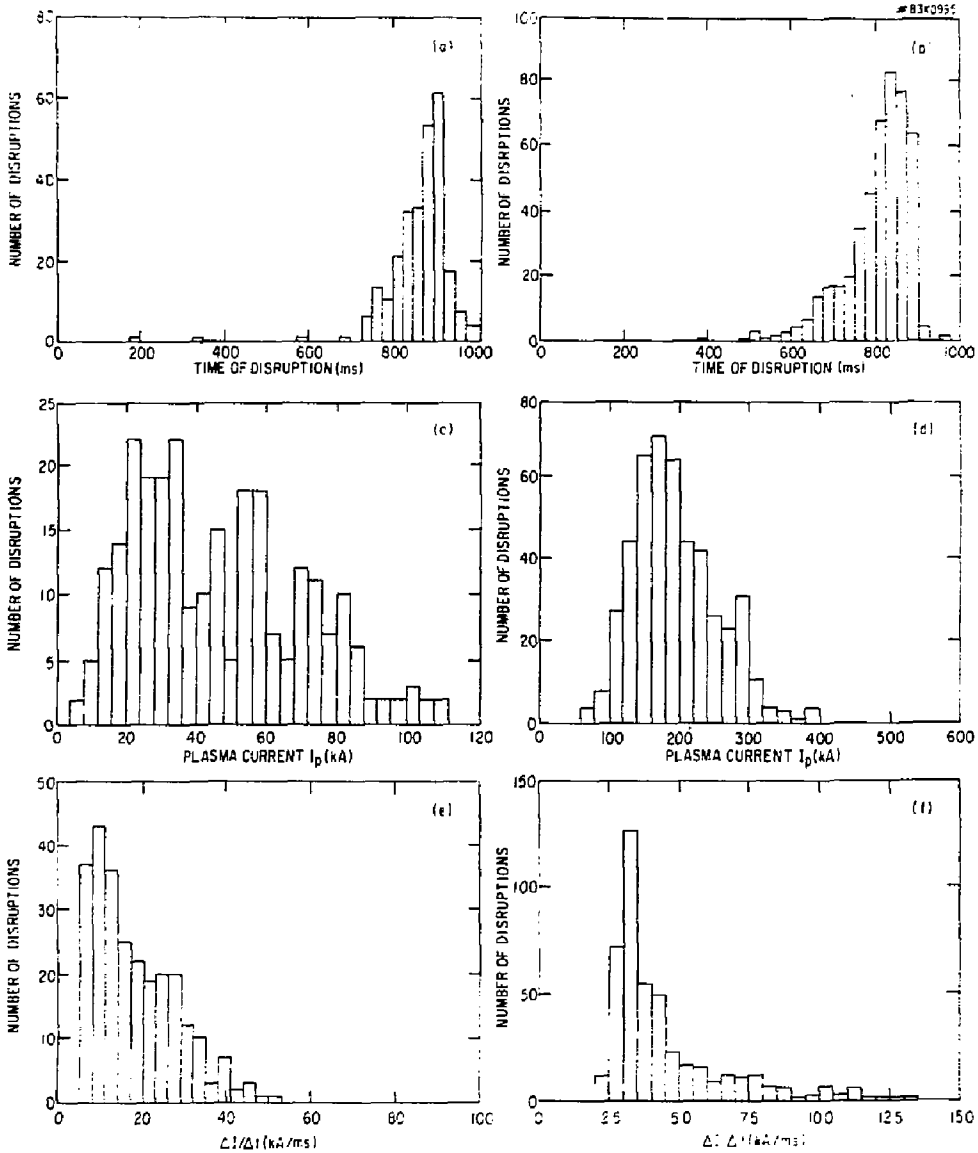
NUMBER OF DISRUPTIONS
TIME OF DISRUPTION (ms)
(a)
(b)
(c)
(d)
(e)
(f)
PLASMA CURRENT I_p(kA)
$\Delta I/\Delta t$(kA/ms)

Fig. 6

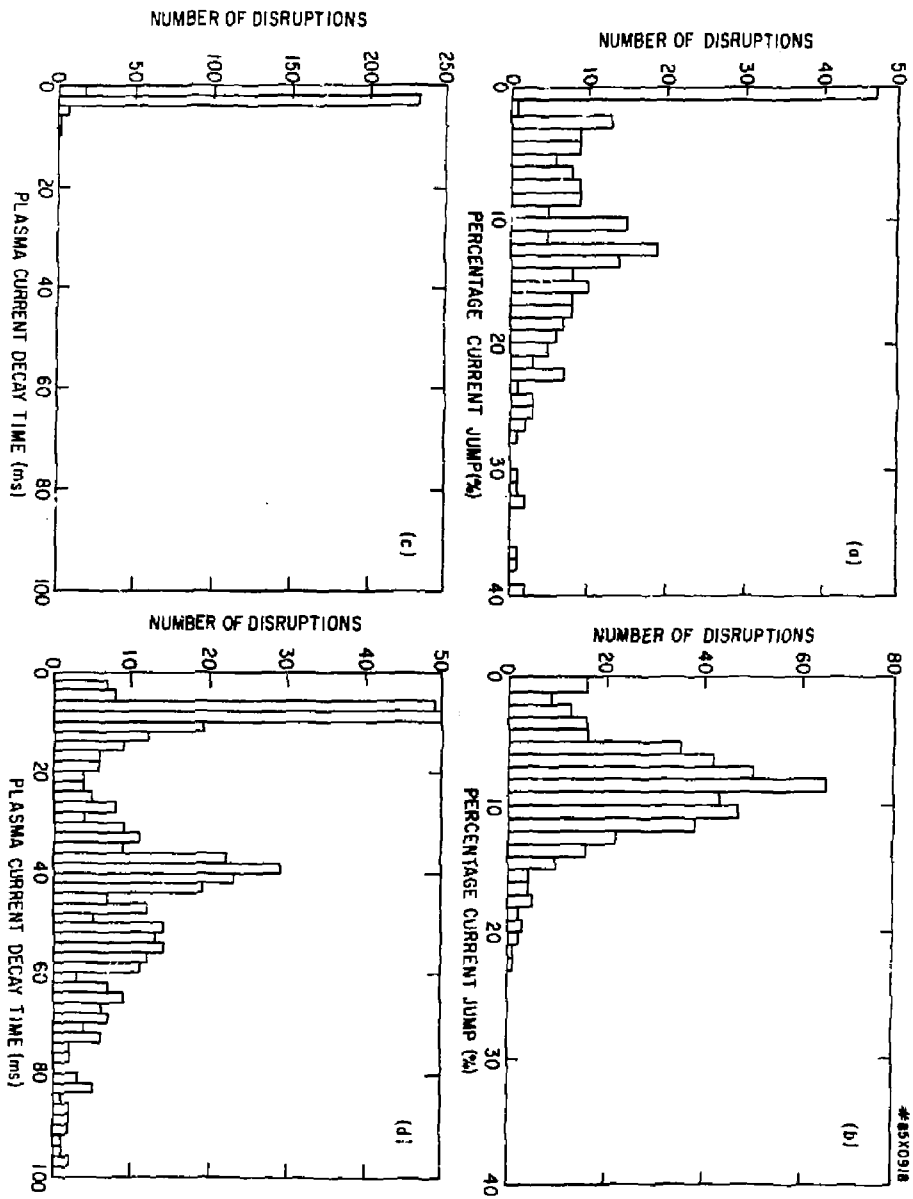
NUMBER OF DISRUPTIONS
PERCENTAGE CURRENT JUMP(%)
(a)
NUMBER OF DISRUPTIONS
PERCENTAGE CURRENT JUMP (%)
(b)
#851091B
NUMBER OF DISRUPTIONS
PLASMA CURRENT DECAY TIME (ms)
(c)
NUMBER OF DISRUPTIONS
PLASMA CURRENT DECAY TIME (ms)
(d)

Fig. 7

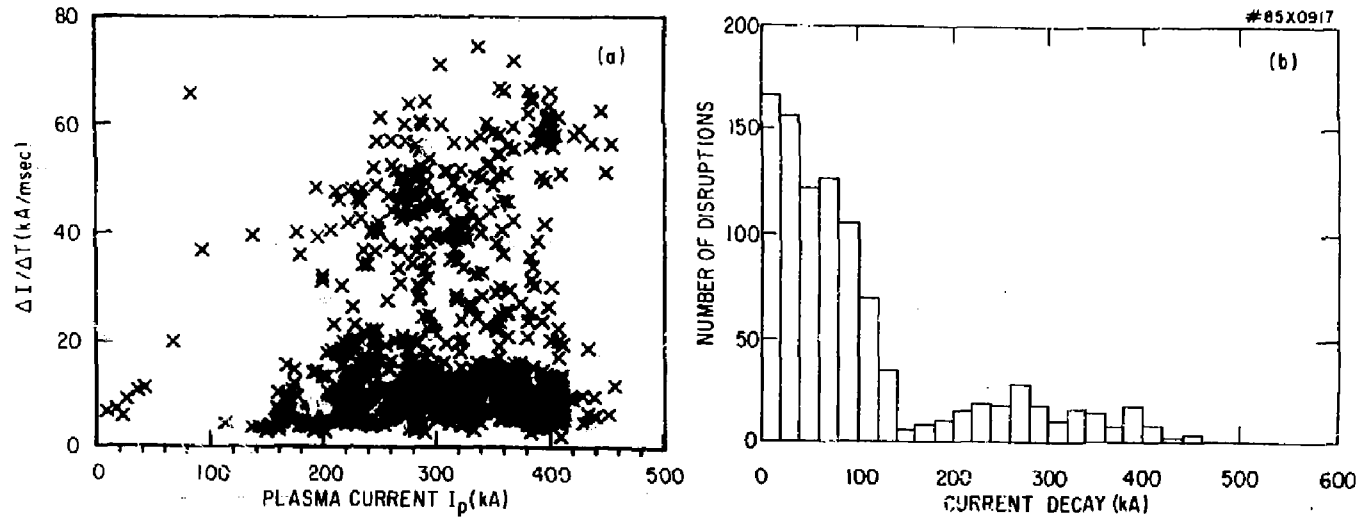
(a)
ΔI/ΔT (kA/msec)
PLASMA CURRENT I_p(kA)
0
20
40
60
80
100
200
300
400
500
#85X0917
(b)
NUMBER OF DISRUPTIONS
CURRENT DECAY (kA)
50
150
600

Fig. 8

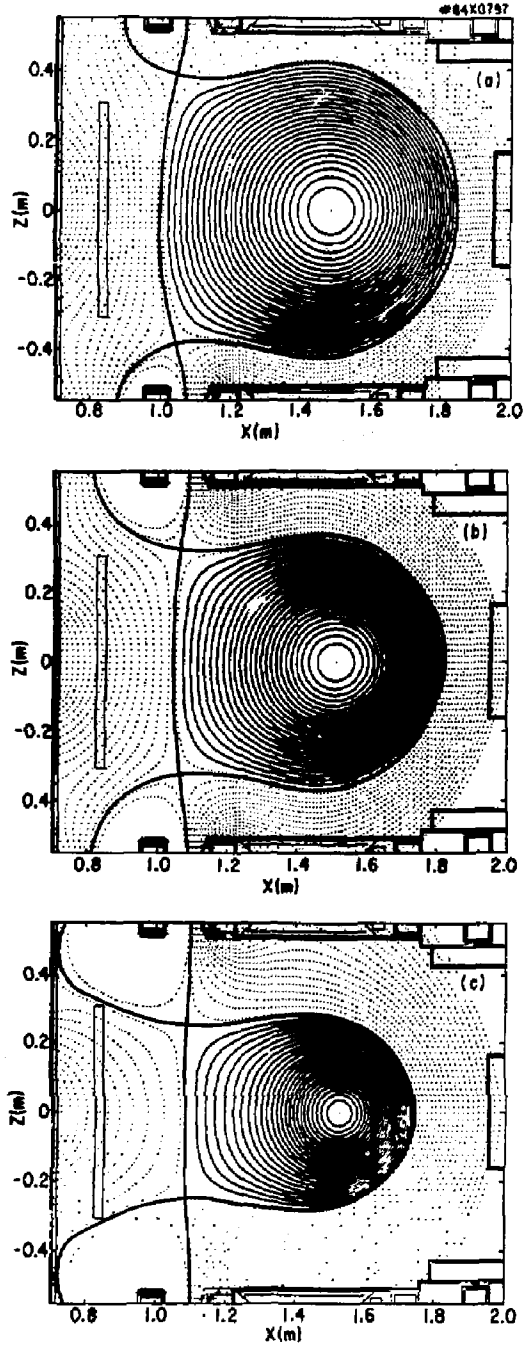

Fig. 9

EXTERNAL DISTRIBUTION IN ADDITION TO UC-20

Plasma Res Lab, Austra Nat'l Univ, AUSTRALIA
Dr. Frank J. Paoloni, Univ of Wollongong, AUSTRALIA
Prof. I.R. Jones, Flinders Univ., AUSTRALIA
Prof. M.H. Brennan, Univ Sydney, AUSTRALIA
Prof. F. Cap, Inst Theo Phys, AUSTRIA
M. Goossens, Astronomisch Instituut, BELGIUM
Prof. R. Boucique, Laboratorium voor Natuurkunde, BELGIUM
Dr. D. Palumbo, Dg XII Fusion Prog, BELGIUM
Ecole Royale Militaire, Lab de Phys Plasmas, BELGIUM
Dr. P.H. Sakanaka, Univ Estadual, BRAZIL
Lib. & Doc. Div., Instituto de Pesquisas Especiais, BRAZIL
Dr. C.R. James, Univ of Alberta, CANADA
Prof. J. Teichmann, Univ of Montreal, CANADA
Dr. H.M. Skarsgard, Univ of Saskatchewan, CANADA
Prof. S.R. Sreenivasan, University of Calgary, CANADA
Prof. Tudor W. Johnston, INRS-Energie, CANADA
Dr. Hannes Barnard, Univ British Columbia, CANADA
Dr. M.P. Bachynski, MPB Technologies, Inc., CANADA
Chalk River, Nucl Lab, CANADA
Zhengwu Li, SW Inst Physics, CHINA
Library, Tsing Hua University, CHINA
Librarian, Institute of Physics, CHINA
Inst Plasma Phys, Academia Sinica, CHINA
Dr. Peter Lukac, Komenskeho Univ, CZECHOSLOVAKIA
The Librarian, Culham Laboratory, ENGLAND
Prof. Schatzman, Observatoire de Nice, FRANCE
J. Radet, CEN-BP6, FRANCE
JET Reading Room, JET Joint Undertaking, ENGLAND
AM Dupas Library, AM Dupas Library, FRANCE
Dr. Tom Mual, Academy Bibliographic, HONG KONG
Preprint Library, Cent Res Inst Phys, HUNGARY
Dr. R.K. Chhajlani, Vikram Univ, INDIA
Dr. B. Dasgupta, Saha Inst, INDIA
Dr. P. Kaw, Physical Research Lab, INDIA
Dr. Phillip Rosenau, Israel Inst Tech, ISRAEL
Prof. S. Cuperman, Tel Aviv University, ISRAEL
Prof. G. Rostagni, Univ Di Padova, ITALY
Librarian, Int'l Ctr Theo Phys, ITALY
Miss Ciella De Palo, Assoc EURATOM-ENEA, ITALY
Biblioteca, del CNR EURATOM, ITALY
Dr. H. Yamato, Toshiba Res & Dev, JAPAN
Direc. Dept. Lg. Tokamak Dev. JAERI, JAPAN
Prof. Nobuyuki Inoue, University of Tokyo, JAPAN
Research Info Center, Nagoya University, JAPAN
Prof. Kyoji Nishikawa, Univ of Hiroshima, JAPAN
Prof. Sigeru Mori, JAERI, JAPAN
Prof. S. Tanaka, Kyoto University, JAPAN
Library, Kyoto University, JAPAN
Prof. Ichiro Kawakami, Nihon Univ, JAPAN
Prof. Satoshi Itoh, Kyushu University, JAPAN
Dr. D.I. Choi, Adv. Inst Sci & Tech, KOREA
Tech Info Division, KAERI, KOREA
Bibliotheek, Fom-Inst Voor Plasma, NETHERLANDS
Prof. B.S. Liley, University of Waikato, NEW ZEALAND
Prof. J.A.C. Cabral, Inst Superior Tecn, PORTUGAL
Dr. Octavian Petrus, ALI CUZA University, ROMANIA
Prof. M.A. Hellberg, University of Natal, SO AFRICA
Dr. Johan de Villiers, Plasma Physics, Nucor, SO AFRICA
Fusion Div. Library, JEN, SPAIN
Prof. Hans Wilhelmson, Chalmers Univ Tech, SWEDEN
Dr. Lennart Stenflo, University of UMEA, SWEDEN
Library, Royal Inst Tech, SWEDEN
Centre de Recherchesen, Ecole Polytech Fed, SWITZERLAND
Dr. V.T. Tolok, Kharkov Phys Tech Ins, USSR
Dr. D.D. Ryutov, Siberian Acad Sci, USSR
Dr. G.A. Eliseev, Kurchatov Institute, USSR
Dr. V.A. Glukhikh, Inst Electro-Physical, USSR
Institute Gen. Physics, USSR
Prof. T.J.M. Boyd, Univ College N Wales, WALES
Dr. K. Schindler, Ruhr Universitat, W. GERMANY
ASDEX Reading Rm, IPP/Max-Planck-Institut fur Plasmaphysik, F.R.G.
Nuclear Res Estab, Julich Ltd, W. GERMANY
Librarian, Max-Planck Institut, W. GERMANY
Bibliothek, Inst Plasmaforschung, W. GERMANY
Prof. R.K. Janev, Inst Phys, YUGOSLAVIA